

Electrochemical approach for the definition of the Pedefferri's diagrams of stainless steels

A. Azimi Dastgerdi¹, F. Bolzoni², A. Brenna³, G. Fumagalli⁴, M. Ormellese⁵, M.P. Pedefferri⁶

¹*Politecnico di Milano, Dipartimento di Chimica, Materiali e Ingegneria Chimica "Giulio Natta", Milan, Italy, arash.azimi@polimi.it*

²*Politecnico di Milano, Dipartimento di Chimica, Materiali e Ingegneria Chimica "Giulio Natta", Milan, Italy, fabio.bolzoni@polimi.it*

³*Politecnico di Milano, Dipartimento di Chimica, Materiali e Ingegneria Chimica "Giulio Natta", Milan, Italy, andrea.brenna@polimi.it*

⁴*Politecnico di Milano, Dipartimento di Chimica, Materiali e Ingegneria Chimica "Giulio Natta", Milan, Italy, gabriele.fumagalli@polimi.it*

⁵*Politecnico di Milano, Dipartimento di Chimica, Materiali e Ingegneria Chimica "Giulio Natta", Milan, Italy, marco.ormellese@polimi.it*

⁶*Politecnico di Milano, Dipartimento di Chimica, Materiali e Ingegneria Chimica "Giulio Natta", Milan, Italy, mariapia.pedefferri@polimi.it*

Abstract

The Pedefferri's diagram of stainless steels aims to define corrosion and passivity (perfect and imperfect conditions) as a function of the imposed potential and chloride content. The conditions can be obtained by determination of pitting and repassivation potentials by means of proper experimental methods. In this work, initiation of localized corrosion was evaluated by localized corrosion potential measurement by means of anodic potentiodynamic polarization test. Two kinds of sample holder were used in order to compare the effect of sample holder geometry on the occurrence of localized corrosion. One of them was according to the ASTM standard and the other one has a different geometry. Also the effect of sample orientation (horizontal or vertical) and surface area was investigated as well. The results showed that localized corrosion initiation depends on the sample holder configuration and sample geometry because of the presence of crevice zones. Moreover, for specimens of 2 cm² and 4 cm² the dominant mechanism of localized corrosion was pitting, however, for 1 cm² the dominant mechanism was crevice corrosion due to the higher perimeter to surface area ratio. Finally, the sample direction changes did not show considerable differences in terms of localized corrosion potential.

Key words: Potentiodynamic test, stainless steel, electrochemical methods, localized corrosion.

Introduction

Chloride-induced corrosion (pitting and crevice corrosion) of stainless steels is considered the main concern in the industrial applications and takes place in the presence of oxygen and chlorides over a critical threshold [1]. Pitting and crevice are unpredictable regarding the initiation of corrosion and corrosion propagation, which occurs with high corrosion rate due to the unfavourable cathodic-to-anodic surface ratio.

In order to understand the corrosion behaviour of stainless steels in chloride containing environment, the Pedefferri diagram is proposed. This diagram is a corrosion map that reports potential with respect to the chloride content in the electrolyte. Pietro Pedefferri initially proposed this diagram for chloride-induced corrosion of carbon steel in concrete. Nowadays, the diagram is reported by the European standard on cathodic protection and prevention for concrete [2-4]. In particular, the diagram (Fig. 1) reports the corrosion condition defined by pitting potential that is the potential over which localized corrosion take place on the material. Two passivity regions are defined: perfect and imperfect zones. Imperfect passivity is the region in which corrosion process cannot initiate but can propagate if already started, while in perfect passivity zone corrosion process can neither initiate nor propagate. These two regions are divided by the repassivation potential, as defined by M. Pourbaix [5]. Finally, immunity and hydrogen evolution zones where corrosion cannot take place for thermodynamic reasons and where hydrogen evolution and consequently hydrogen embrittlement of high strength steel can take place. The goal of this paper is part of a research in which we want to extend the Pedefferri diagram of carbon steel in concrete to stainless steel in chloride containing solution in order to obtain an engineering tool indicating the corrosion behaviour of these materials. In order to extend the diagram to stainless steels, it is essential to find the most reliable electrochemical method to determine pitting and repassivation potentials (E_{pit} and E_{rep} , respectively), since the value of these potentials depends on the adopted method [6]; moreover, reproducibility of the data obtained for localized corrosion potential is poor due to the fact that it is stochastic phenomenon [7, 8]. Localized corrosion and repassivation potentials depend on different parameters such as metallurgical and environmental factors (steel chemical composition, chloride content, pH, temperature, presence of inclusions, surface finishing, etc.). Different electrochemical methods have been used for the evaluation of the pitting corrosion resistance of stainless steels. Some researchers used localized electrochemical techniques such as Scanning Electrochemical Microscopy (SECM) [9] and electrochemical noise [10]. However, the most researches in this field are focused on the measurement of anodic polarization curve [11, 12]. Pitting potentials can be rapidly measured by the galvanostatic anodic polarization method [13], which has claimed avoiding crevice corrosion during determination of pitting potential. Potentiostatic and potentiodynamic are the most used techniques to determine E_{pit} and E_{rep} , although it is stated that both of them have advantages and disadvantages. In former case the test is time consuming, but has more precise results as well as determination of critical chloride content, however, the latter case is fast, but the results depends on the scan rate to a great extent [14-20]. It seems that using these two methods in order to determine E_{pit} and E_{rep} would be useful to have more reliable results. However, according to standard ASTM G 61, the most common electrochemical technique used for determining such pit potentials is the cyclic potentiodynamic anodic polarization test [21].

In this paper, potentiodynamic test is used, as the starting method, to determine the concerned features of localized corrosion. This kind of test can be compare in the future with other different tests as potentiostatic and galvanostatic which are not proposed in this paper. Potentiodynamic tests were carried out in order to study different conditions. First of all, the effect of sample geometry is assessed. In this stage, the ASTM sample holder (configuration No. 1) is compared with a proposed configuration (configuration No. 2) of sample with a

different geometry as it will describe in the experimental procedure. Moreover, the effect of the size of the exposed surface and sample orientation on localized corrosion initiation is studied.

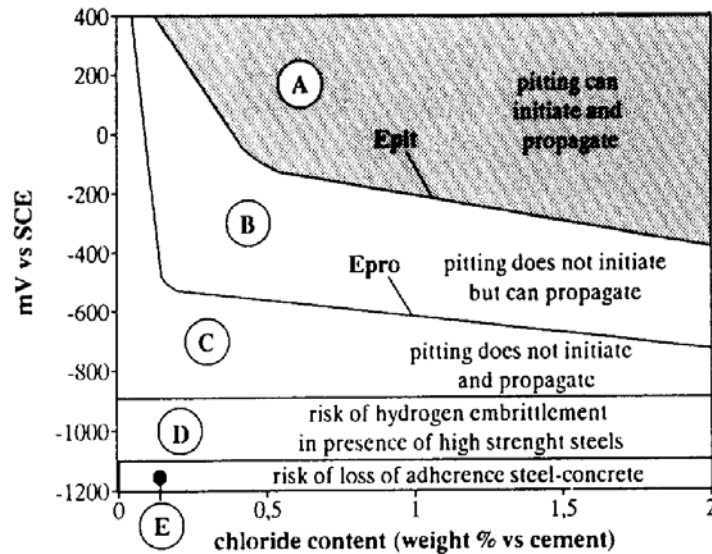


Figure 1– Pedefferri's diagram of steel in concrete as reported in [2].

Experimental procedure

Tests were carried out on austenitic stainless steel AISI 304L. Table 1 reports steel chemical composition. In sample preparation stage, after cutting, specimens prepared using abrasive papers from 120 to 1200 grits and then the surfaces cleaned with acetone. Samples used for the experiments had two different geometry with respect to the kind of sample holder.

Two types of sample holder configurations have been used:

Configuration No. 1: this is the ASTM standard sample holder in which stainless steel specimens were cut from a bar and placed in a PTFE cylindrical sample holder (Figure 2a) made of two watertight caps, in order to expose to the electrolyte a circular area of 1 cm². A polymeric O-ring is interposed between the specimen and the sample holder. A metal rod was screwed in a hole on the top of the sample holder to provide the electrical contact with the specimen inside the cap. In order to prevent the contact between the metal rod and the surrounding environment, a glass tube was placed around the screw and was pressed against the sample holder interposing an O-ring joint between them.

Configuration No. 2: this sample holder is supposed to limit the crevice effect [22]. Samples were cut from plates in 2 x 3 cm size. In this sample holder, brazed joints were used for the electrical contact and an auxiliary mask was applied on the surface with the aim to obtain an exposed areas of 1 ± 0.05 cm², 2 ± 0.05 cm² or 4 ± 0.05 cm². The specimen was inserted in the holder (polycarbonate tube) in a vertical or horizontal position depending the orientation need to be test; it was fixed to it with an anti-corrosive silicon sealant, which also help to isolate the electrical contacts. Before silicon polymerization, the auxiliary mask was removed and after silicon polymerization, manual cleaning of the exposed surface using acetone and visual inspection using a microscopy have done in order to discard the specimens with defects (e.g. smears of silicon or low adherence of the silicone shield). Fig. 2b shows a typical proposed sample holder with silicon and plastic tube.

Potentiodynamic tests were used to determine the features of localized corrosion. The tests were carried out using potentiostat EG&G Princeton applied research model 273A and NaCl

solution with the concentration of $28 \times 10^{-3} \text{ mol}\cdot\text{L}^{-1}$ ($1000 \text{ mg}\cdot\text{L}^{-1}$) chloride, at room temperature ($T = 25 \pm 1 \text{ }^{\circ}\text{C}$), pH 6. The potential scan rate is 0.166 mV/s according to the standard [23]. Table 2 reports the experimental conditions for the different specimens used for the experiment. The potential was measured with a Ag/AgCl/KCl_{sat.} reference electrode placed in a glass Luggin capillary in order to avoid the ohmic drop contribution in the potential measurement. An inert activated titanium counter electrode with 10 cm^2 surface area was used.

Table 1- Chemical composition of AISI 304 L

| Element | Cr | Ni | Mn | Si | Cu | Mo | N | P | C | S | Fe |
|-------------|--------|-------|-------|-------|-------|-------|-------|-------|-------|-------|--------|
| % by weight | 17,271 | 8,422 | 1,458 | 0,372 | 0,361 | 0,076 | 0,063 | 0,033 | 0,018 | 0,003 | 71,899 |

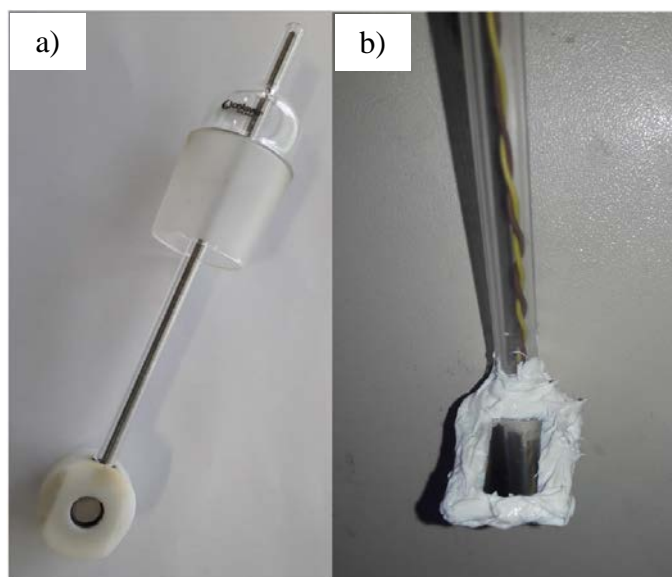


Figure 2- Sample holders, a) configuration No. 1, b) configuration No. 2.

Table 2- Experimental conditions for different specimens

| Sample holder | Number of specimen | Sample orientation | Surface area |
|---------------------|--------------------|--------------------|------------------|
| Configuration No. 1 | 10 | Vertical | 1 cm^2 |
| Configuration No. 2 | 5 | Horizontal | 1 cm^2 |
| Configuration No. 2 | 5 | Horizontal | 2 cm^2 |
| Configuration No. 2 | 5 | Vertical | 2 cm^2 |
| Configuration No. 2 | 5 | Horizontal | 4 cm^2 |

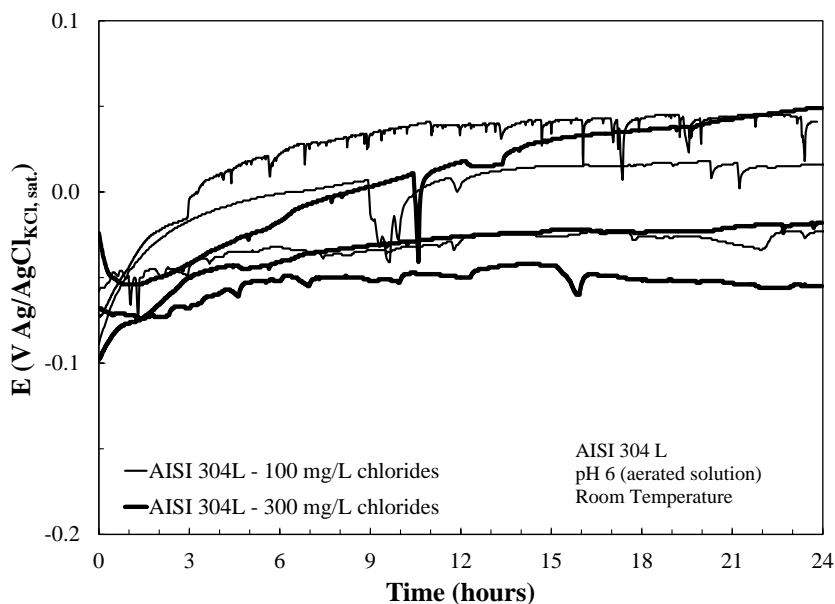
Results and Discussion

Measurement of pre-conditioning time

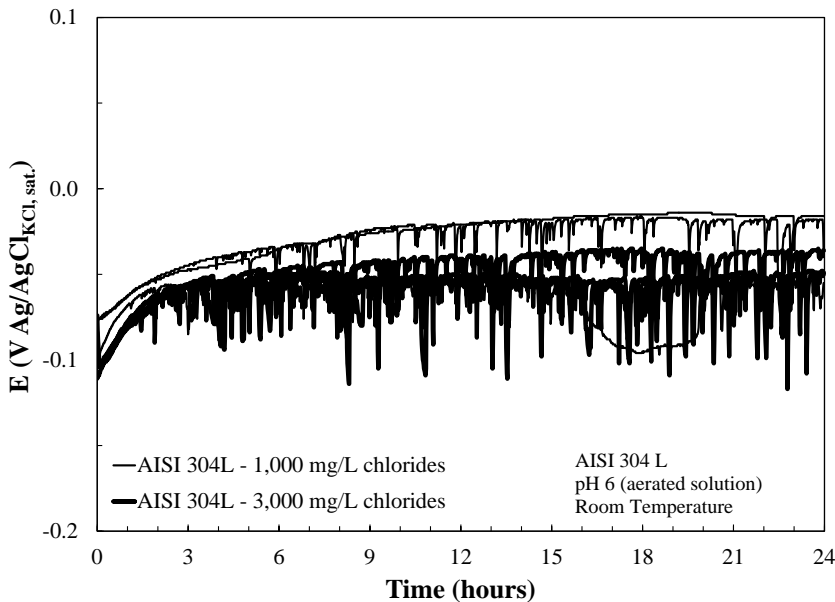
In order to select the pre-conditioning time for the specimens in solution before testing, free corrosion potential (E_{corr}) versus time measurements have been carried out for different chloride concentrations which are 100, 300, 1000 and $3000 \text{ mg}\cdot\text{L}^{-1}$ (Figures 3a and 3b). After the immersion of the specimen in solution, the potential was monitored for 24 hours.

As can be seen in Fig. 3a, there are some oscillations in the graphs for both 100 and $300 \text{ mg}\cdot\text{L}^{-1}$ but for the 1000 and $3000 \text{ mg}\cdot\text{L}^{-1}$ (Fig. 3b), the oscillations are severe. Oscillations can

be probably due to the formation of some metastable localized corrosion phenomenon which means that probably some pits or crevice attack start and immediately repassivate [24]. According to the graphs, the potential variation is about 50 mV in the first 6 hours after immersion and then become stable; accordingly, the stable condition where the potentials start to be constant with respect to the time is between 6 to 24 hours. Therefore, in order to be confident that the specimens have formed stable passive layer, the 24 hours pre-conditioning time is selected for all potentiodynamic tests.



a)



b)

Figure 3- Potential versus time graphs for the determination of pre-conditioning time, a) for 100 and 300 $\text{mg}\cdot\text{L}^{-1}$ chlorides, b) for 1000 and 3000 $\text{mg}\cdot\text{L}^{-1}$ chlorides.

Effect of sample holder configuration

Fig. 4 shows the results of cyclic potentiodynamic tests for stainless steel 304 L sample in configuration No. 1 (ASTM Standard sample holder). Results show that free corrosion potential is between -0.1 and 0.1 (V Ag/AgCl_{KCl,sat}) which is the same range according to corrosion potential versus time results in Fig. 3. The first part of the curve corresponds to the passive range and passive current density is in the order of 0.1 to 3 mA/m² which is the typical value of passive current density. After reaching to the potential of about 0.2-0.3 (V Ag/AgCl_{KCl, sat}) a sharp increase in the current density can be observed which means that localized corrosion take place on the sample. When the curve reach a critical current, the reverse scan would start in order to measure the repassivation potential. All the graphs show oscillations in the passive current range and the points in which the current density starts to increase are different for each curves and range between 0.16 and 0.30 (V Ag/AgCl_{KCl,sat}). As it mentioned before, the observed oscillations can be probably due to the formation of some metastable localized corrosion phenomenon. In some graphs, it is difficult to determine not only the point for starting localized corrosion but also the repassivation potential, because of the oscillations that make hard the recognition of these points. Moreover, from the observations of the specimens after tests (Fig. 5a), it is revealed that there are corrosion lines on the specimens located exactly in the contacting point of O-ring with specimen and solution which refers to the crevice phenomenon, although by stereomicroscope one can observe very small pits that is impossible to see with naked eye (Fig.5b). The scatter of the data in Fig. 4 is to some extent due to the crevice corrosion that readily develops in shielded areas at specimen/holder interface during potentiodynamic measurements [7, 8].

Crevice is easily identifiable because it reveals with a gradual increase of the corrosion current during the forward polarization, usually distinct from the sharp current increase due to pitting and occurring at much lower potentials. After reversing the potential, the anodic current remains high or continues to slightly increase depending on the extent of crevice propagation that has occurred [7]. Fine crevices may be also the result of a preferential nucleation of pits at specimen/holder (or specimen/mounting material) interfaces (referred as the heterogeneous pit to distinguish it from the normal or homogeneous pit). When this form of pit grows, it resolves as a groove much like a crevice [25]. In the event of heavy crevice, the reverse cathodic scan may even fail to obtain any pit or crevice repassivation [12].

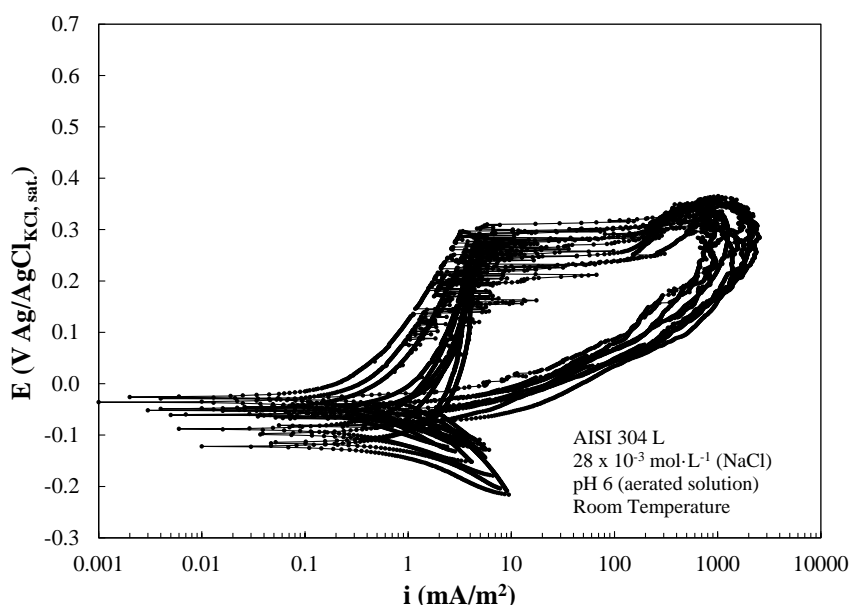


Figure 4- Potentiodynamic tests for the specimens with 1 cm² surface in configuration No. 1.

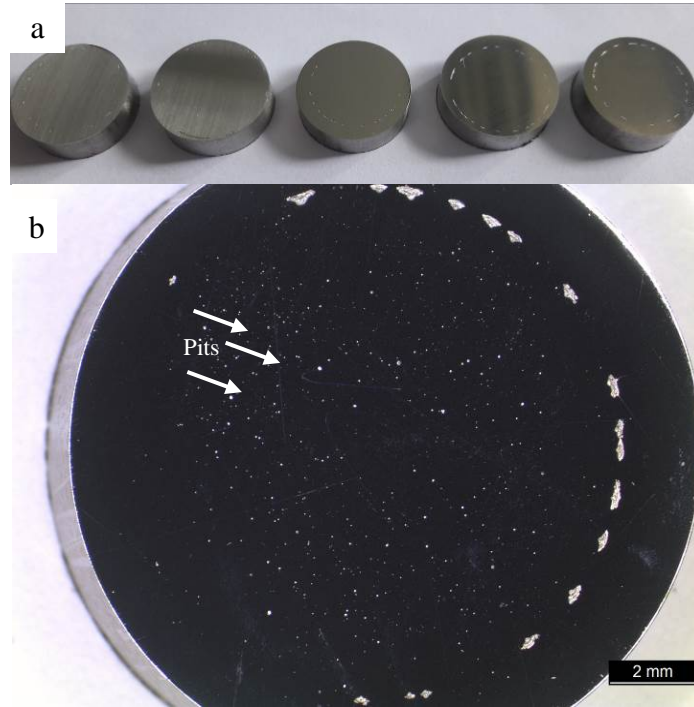


Figure 5- Crevice corrosion in configuration No. 1 samples, a) crevice corrosion areas in different specimens, b) stereomicroscope image of crevice along with very small pits.

Potentiodynamic results for the specimens with 1 cm^2 , 2 cm^2 and 4 cm^2 surface areas for horizontal condition and 2 cm^2 for vertical condition with using configuration No. 2 (proposed sample holder) have shown in Figures 6, 7, 8 and 9, respectively. According to the results, the curves in these figures are more stable and metastable phenomenon and oscillations are very low with respect to the configuration No. 1. Localized corrosion potentials of configuration No. 1 are far below in compare with the specimens of configuration No. 2. Moreover, the passive current density is very stable and is between $1\text{-}5 \text{ mA/m}^2$ and free corrosion potential is in the same range with the results of corrosion potential versus time in Fig. 3. From the results, it seems that the corrosion potential is not influenced by geometry, nevertheless, the localized corrosion potential can be different according to the kind of configurations.

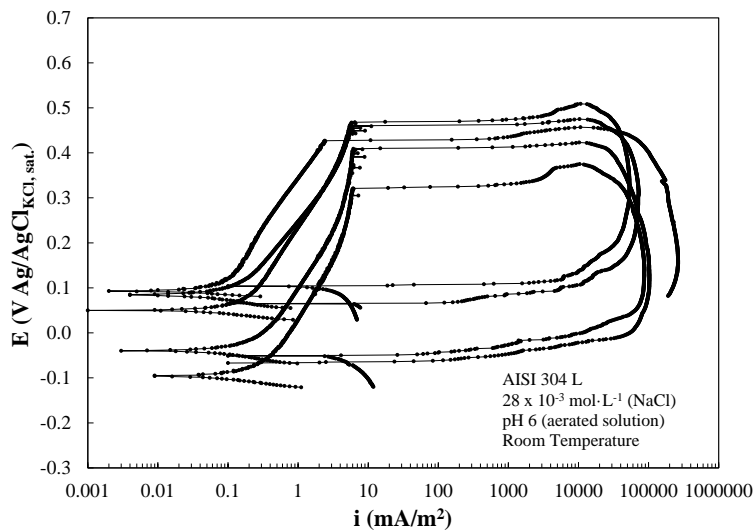


Figure 6- Potentiodynamic tests for the configuration No. 2 specimen, with 1 cm^2 surface area with horizontal direction.

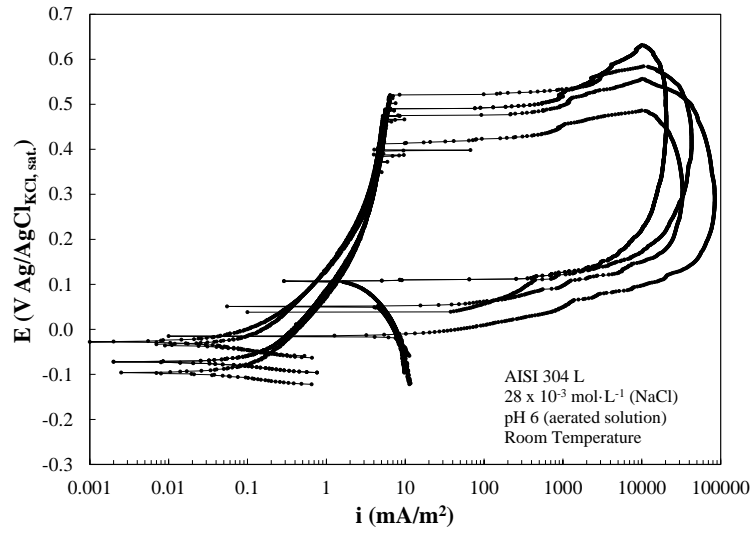


Figure 7- Potentiodynamic tests for the configuration No. 2 specimens, with 2 cm² surface area with horizontal direction.

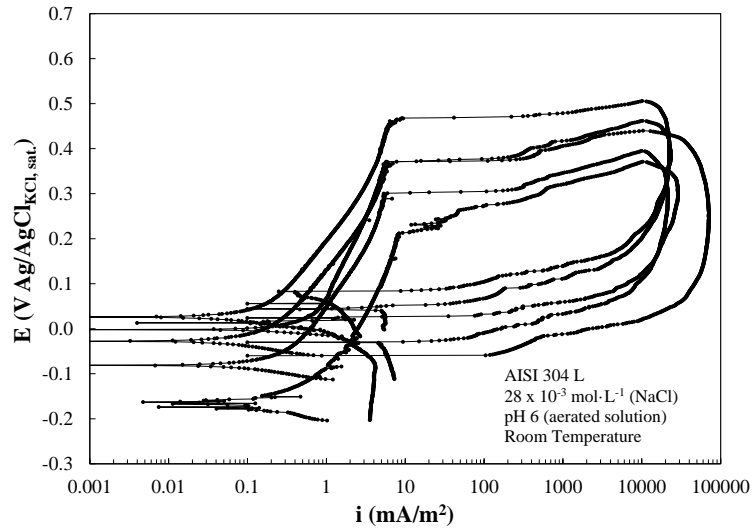


Figure 8- Potentiodynamic tests for the configuration No. 2 specimens, with 4 cm² surface area with horizontal direction.

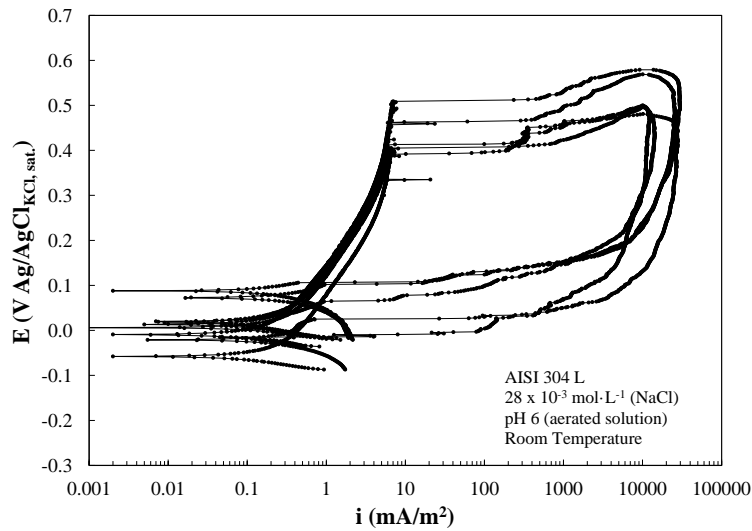


Figure 9- Potentiodynamic tests for the configuration No. 2 specimens, with 2 cm² surface area with vertical direction.

Fig. 10 shows the difference in localized corrosion potentials among different specimens with different configurations. The Figure reports the number of corroded specimen (in percentage) with respect to the localized corrosion potential measured according to the potentiodynamic curves. As can be seen, about 60 percent of the specimens for configuration No. 1 have localized corrosion potentials lower than or equal to +0.3 (V Ag/AgCl_{KCl,sat}), while the other samples (configuration No. 2) have the potentials between 0.3 and 0.5 (V Ag/AgCl_{KCl, sat}). This results confirm the negative effect of crevice corrosion on the occurrence of localized corrosion. Figures 11 and 12 show the difference in corrosion potentials and repassivation potentials among different specimens, respectively. As it can observe, there are no remarkable differences among all specimens in terms of corrosion and repassivation potentials which means that both of them are not strongly influenced by geometry.

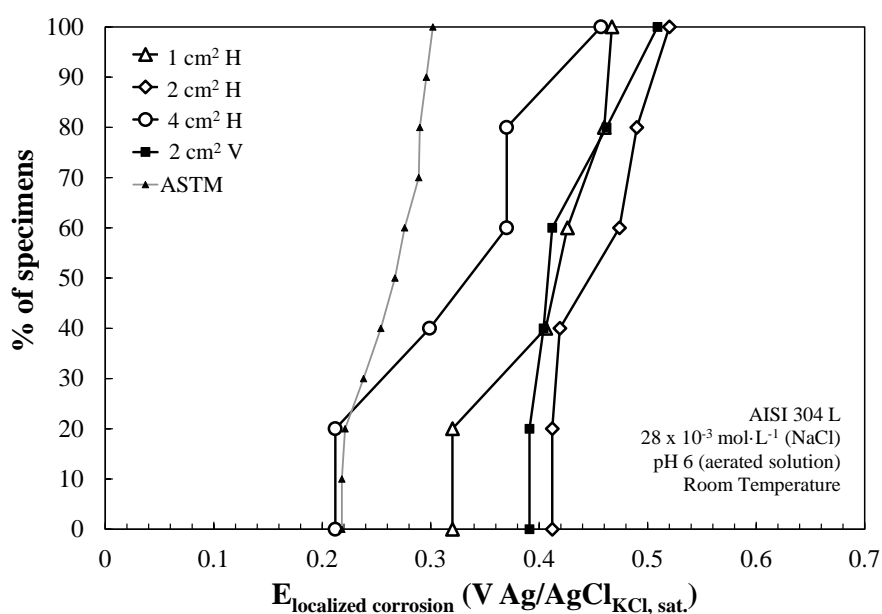


Figure 10- Number of corroded specimens with respect to the localized corrosion potentials of the samples.

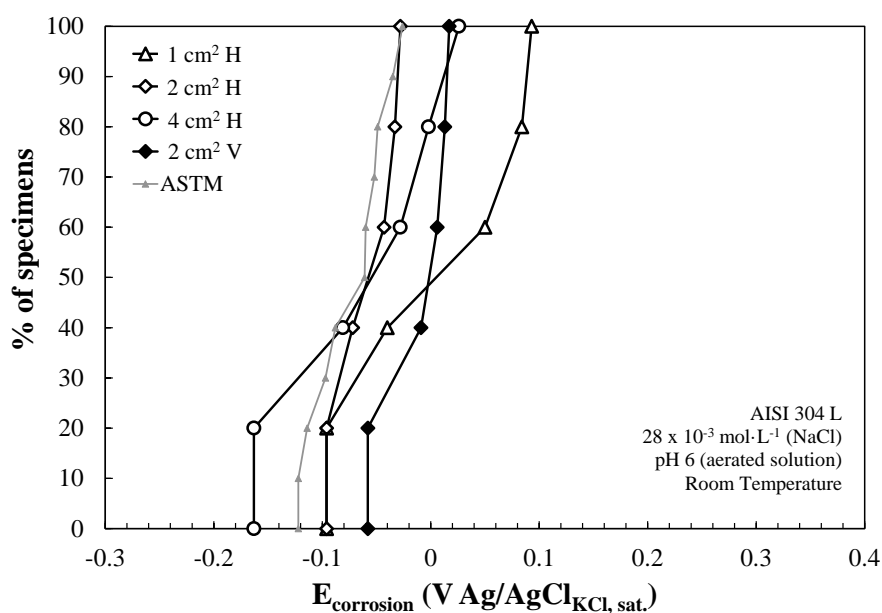


Figure 11- Number of corroded specimens with respect to the corrosion potentials of the samples.

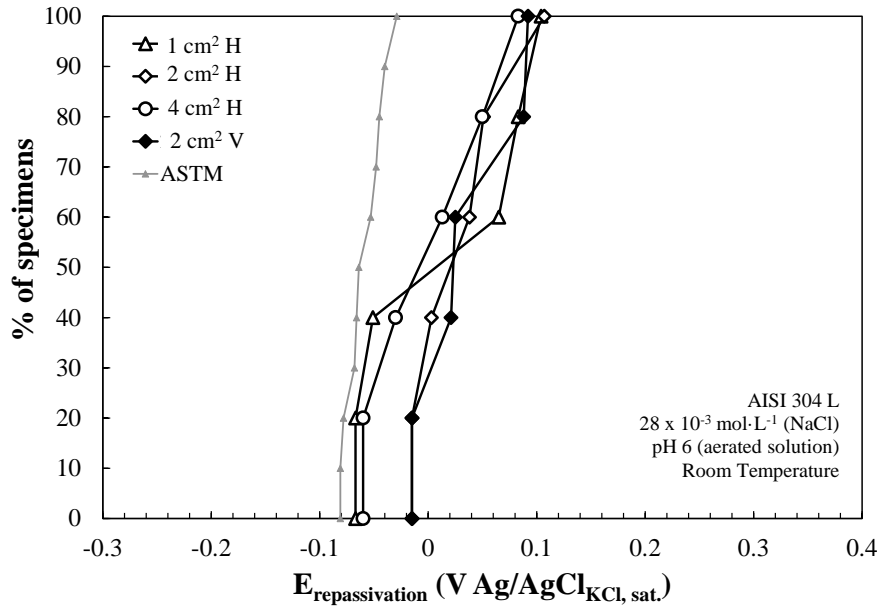


Figure 12- Number of corroded specimens with respect to the repassivation potentials of the samples.

Effect of sample orientation

Sample orientation is evaluated by comparing the specimens of 2 cm² with horizontal and vertical directions. The results do not show considerable differences in localized corrosion potentials and data are in the same range (Fig. 10). Although the evaluation of the effect of sample direction by potentiostatic measurement in some researches [22] have shown that samples with horizontal direction have more vulnerable and sensitive condition to localized corrosion in aggressive solutions, it is important to note that in potentiodynamic test the time may not be enough to see a clear and recognizable effect of the sample direction of localized corrosion initiation.

Effect of surface area

Comparison among the specimens with different surface areas and the same orientation (horizontal), show that specimens with 4 cm² surface area, reach to the localized corrosion point in lower potentials in compared with the others (Fig. 10). It also can be seen in Fig. 13, where the localized corrosion potential is plotted with respect to the surface area and perimeter to surface ratio of the specimens. In this graph, the mean values of each group of samples with different surface areas are considered as a criterion for evaluating the trend. As one can see, the localized corrosion potential has a maximum for 2 cm² surface area and decreases for surface area of 4 cm² according to the effect observed in [26, 27]. The lower value is about +0.3 (V Ag/AgCl_{KCl, sat.}) for 4 cm² and is surprising to have a lower value at the 1 cm². The interpretation of this kind of trend can be related to the presence of crevice corrosion in the smaller specimens. For this reason, it is graphed not only localized corrosion potential with respect to the surface but also with respect to the ratio between the perimeter and the surface of the sample. Our interpretation is that the small surface of the sample introduces the higher crevice effect due to the high perimeter-to-surface ratio. Therefore, in lower ratios, the perimeter would be lower with respect to the surface area and in this case, the probability of crevice corrosion would reduce. From this perspective, it can be construed that from specimens of 4 cm² to 2 cm², the dominant mechanism is the creation of pitting on the surfaces which will increase with the increase of the surface areas. However, in the specimens

of 1 cm² the dominant mechanism is the creation of crevice corrosion due to the high perimeter to surface area ratio.

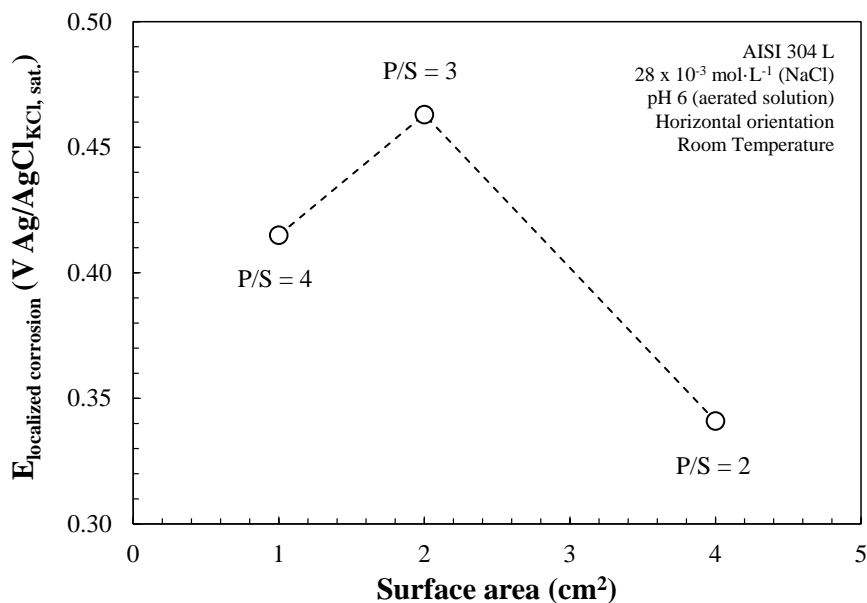


Figure 13- Comparison among different specimens of configuration No. 2 in horizontal direction in terms of surface area and perimeter to surface ratio (P/S).

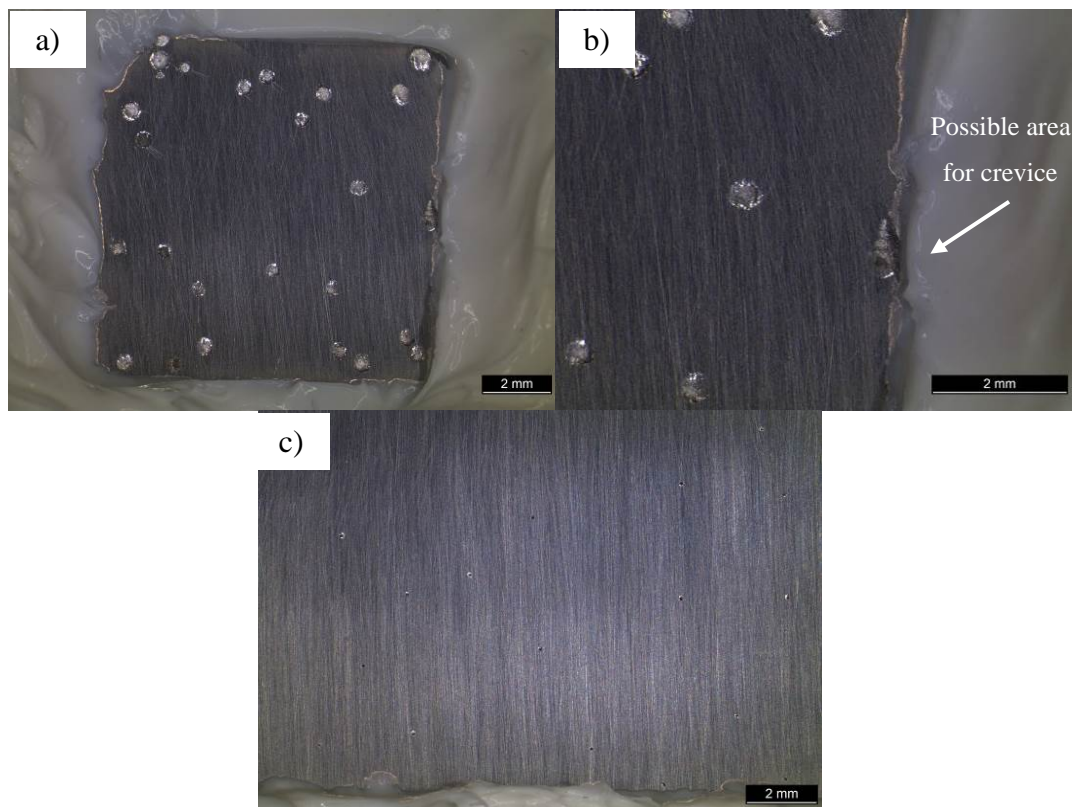


Figure 14- Stereographic image of pitting in the specimen of 1 cm² and 4 cm² horizontal, a) whole of the specimen with 1 cm², b) edge of the specimen with 1 cm², c) specimen with 4 cm² surface area.

The pictures have taken by stereographic microscope from the specimens with different surface areas promoted the aforementioned assumption about the crevice and pitting behavior of the specimens with different perimeter to surface area ratio. Figure 14 show the localized corrosion condition of the specimens with 1 cm² and 4 cm² surface area. As can be seen, the amount of pits in the 1 cm² specimen (Fig. 14a) is lower than that in 4 cm² specimen (Fig. 14c), nevertheless, the size of pits in former is bigger than the latter case. By focusing on the interface of silicon and metal in the edges of specimen, it is likely to see the areas in the interfaces of metal and silicon which can be crevice corrosion (Fig. 14b). It is important to note that, the occurrence of crevice corrosion is inevitable apart from the size of specimen or the kind of sample holder, but the severity of this kind of localized corrosion can be different according to geometry of the sample. In this case, it was supposed that the severity of the crevice corrosion is higher for 1 cm² specimens in compared with 2 cm² and 4 cm² specimens which is in good agreement with the results obtain in Fig. 13.

Conclusion

Potentiodynamic polarization tests were carried out in order to study localized corrosion behavior of austenitic stainless steel AISI 304L in chloride-containing solution.

In order to find the best condition to evaluate localized corrosion characteristic of the material, ASTM standard sample holder (Configuration No. 1) and a proposed sample holder (configuration No. 2) were compared. The results showed that the configuration No. 1 is more prone to crevice corrosion in compared with the proposed type of sample holder. Furthermore, the existence of crevice corrosion can affect the anodic curve either with decreasing the potential to reach localized corrosion before pitting take place or the shape of the curve with sever oscillations. Sample geometry has poor influence on corrosion and repassivation potential of the specimens.

Potentiodynamic tests on specimens with different surface area (1 cm², 2 cm² and 4 cm²) revealed that the more the exposed surface area, the less the potential in which the metal reach to the localized corrosion and dominant mechanism is mainly based on the pitting. Conversely, the localized corrosion potential of 1 cm² specimens dropped due to the existence of crevice corrosion and higher perimeter to surface area ratio regarding to other specimens with higher surface areas. The results for different orientations did not show any tangible effect.

References

- [1] G.T. Burstein, R.M. Souto, C. Liu, S.P. Vines, *Corros. Mater.* 29 (2004) S1–S4.
- [2] P. Pedferri, *Construct. Build. Mater.* 10 (1996) 391.
- [3] C. L. Page, “Cathodic Protection of Reinforced Concrete principles and Applications”, in: *Proceeding of International Conference on Repair of Concrete Structures*, (1977) pp. 123-32.
- [4] L. Bertolini, F. Bolzoni, M. Gastaldi, T. Pastore, P. Pedferri and E. Redaelli, *Electrochimica Acta*, 54 (2009) 1452-1463.
- [5] M. Pourbaix, NACE International publication, 1995.
- [6] Z. Szklarska, NACE Publication, (1986).
- [7] L. Bertolini, B. Elsener, P. Pedferri, R. Polder, Wiley VCH, (2004).
- [8] L. Stockert, F. Hunkeler, H. Bohni, *Corrosion*, 41 (1985) 676.
- [9] R. Leiva-García, R. Akid, D. Greenfield, J. Gittens, M.J. Munoz-Portero, J. García-Antón, *Electrochimica Acta*, 70 (2012) 105-111.
- [10] A. Burkert, H. S. Klapper and J. Lehmann, *Materials and Corrosion*, 64 (2013) 675-682.
- [11] Y. Yi, P. Vho, A. Al Zaabi, Y. Addad and C. Jang, *Corros. Sci.*, 74 (2013) 92–97.

- [12] S. Frangini, N. De Cristofaro, *Corros. Sci.*, 45 (2003) 2769–2786.
- [13] Z. Szklarska-Smialowska, M. Janik-Czachor, *Corros. Sci.*, 11 (1971) 901.
- [14] L. Bertolini, M. Gastaldi, *Materials and Corrosion*, 62 (2011) 120–129.
- [15] Y. Zhang, M. Urquidi-Macdonald, G.R. Engelhardt, D.D. Macdonald, *Electrochim. Acta*, 69 (2012) 12–18.
- [16] N. Alonso Fallerios, A. Hakim, S. Wolyneć, *corrosion science section*, 55 (1999) 443–448.
- [17] M. Gastaldi, F. Lollini, L. Bertolini, *EUROCORR corrosion congress*, (2014), 1-9.
- [18] M.C. Alonso, M. Sanchez, *Materials and corrosion*, 60 (2009) 631-637.
- [19] L. Bertolini, E. Redaelli, *Materials and Corrosion*, 60 (2009) 608-616.
- [20] B. Baroux, *Corros. Sci.*, 28 (1988) 989.
- [21] ASTM G 61-86, *Annual Book of ASTM Standards*, 3 (1986) pp. 223–227.
- [22] F. Bolzoni, G. Contreras, G. Fumagalli, L. Lazzari, G. Re, *Corrosion*, 69 (2013) 352-363.
- [23] UNI EN ISO 17475, *EUROPEAN STANDARD*, (2008).
- [24] G.T. Burstein, C. Liu, R.M. Souto, S.P. Vines, *Corros. Eng., Sci. Technol.* 39 (2004) 25–30.
- [25] L. Soria, E.J. Herrera, in: *Proceedings of Eleventh International Corrosion Congress*, (1990) pp. 5–485.
- [26] U. Angst, B. Elsener, C. K. Larsen and O. Vennesland, *2nd International Symposium on Service Life Design for Infrastructure*, (2010) pp. 569-576.
- [27] L. Li, and A.A. Sagüés, *Corrosion*, 60 (2004) 195-202.